



Research article

UDC 626.01

DOI: 10.34910/MCE.123.3




Hoek–Brown model for ice breaking simulation

S.A. Andreeva¹ , D. Sharapov² 

¹ Admiral Makarov State University of Maritime and Inland Shipping, St. Petersburg, Russian Federation

² Peter the Great St. Petersburg Polytechnic University, St. Petersburg, Russian Federation

 Cofiaand16@gmail.com

Keywords: Hoek–Brown model, ice model, ice failure, ice bending, finite-element analysis

Abstract. Arctic is an important region for science and economic projects. New infrastructure is required for the sustainable development of this region. The water transport infrastructure in Arctic is subject to extreme environmental impacts. One of the main loads on such structures is the ice load. Conventional way to assess ice loads is to use empirical equations from normative documents. Nowadays with the increasing complexity of designs the numerical calculations became more important. Modern software and material models become more common in design. Ice model is not incorporated in the common engineering software, therefore engineers have to choose among available models. The Hoek–Brown model of ice is considered as one of the most suitable preinstalled material models in the Plaxis software package. As of today, the authors found no studies proving the applicability of the Hoek–Brown model to the destruction of ice by bending, so this problem is of interest. The Hoek–Brown model was examined by using available results of the field ice bending tests. The authors compared the ice strength from the numerical calculation and field tests. Young's modulus was estimated with Vaudrey equation. The calculation results from Hoek–Brown model showed the possibility of the model application in general case. The convergence of the results was revealed, with an error that in most cases does not exceed 20 %. Bigger discrepancy for some result points can be explained by the presence of the excessive brine volume in ice.

Funding: The project is carried out with the support of the Russian Ministry of Education and Science "Study of statistical patterns of ice loads on engineering structures and development of a new method for their stochastic modeling (FSEG 2020-2021)" No. 0784-2020-0021

Citation: Andreeva, S.A., Sharapov, D. Hoek–Brown model for ice breaking simulation. Magazine of Civil Engineering. 2023. 123(7). Article no. 12303. DOI: 10.34910/MCE.123.3

1. Introduction

The development of the Arctic territories is one of the priorities for scientific research and economic development. It is important for a number of reasons: rich deposits of minerals, natural resources of animal and plant origin, traffic routes (including Europe–Asia), climate study, and others. Meanwhile, construction in harsh Arctic conditions inevitably faces a number of challenges, primarily related to low temperatures and ice impacts. The transport infrastructure of the Arctic region in some areas is inevitably limited to sea and river ports. These berthing complexes are subject to considerable ice loads and must be designed against ice actions. To determine ice loads in the modern world, software programs are usually used. Not all programs have a wide range of material models, so it is important to understand the possibilities of replacing complex ice models with simple standard ones. Plaxis is widely used by hydraulic engineers, but it does not have a special ice model. The object of the investigation is to evaluate the applicability of the most suitable material model in the Plaxis program (Hoek–Brown model) for modeling of the ice destruction by bending.

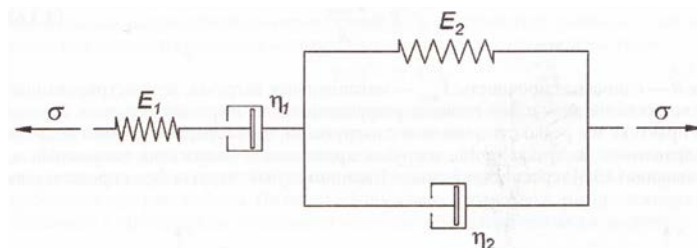
The calculation of ice loads is usually carried out with the help of normative documents [1-4], and can be confirmed by modeling. Computer modeling of ice as a material is a separate problem in software systems [5-7] and usually, the material "ice" is not in the database of popular engineering calculation systems [8, 9]. The user is invited to select the general model and introduce the characteristics of ice for the given calculation tasks. The relevance of the topic of this work is related to the lack of verification data about the Hoek–Brown model for breaking ice by bending in the Plaxis software package. The breaking of ice by bending is the subject of many articles describing the theoretical approach to determining strength [10-15], as well as physical field experiments [12]. The modeling of ice failure by bending is described in detail in the work of L. Li [15]. L. Li carried out strength analyses and comparisons with D.S. Sodhi experiments [13] to calculate ice loads on ocean and marine hydrotechnical constructions. The authors used a dynamic approach to modeling ice destruction using the LS-Dyna program. This approach deserves attention but uses a different problem statement as well as models that are not available in the Plaxis software package. The work of S.V. Godetsky on the assessment of ice strength in the Sea of Okhotsk [16] deserves a special attention as it well describes the strength properties of ice. However, the Hoek–Brown model is not considered in the work by S.V. Godetsky. The authors O.V. Yakimenko and S.A. Matveev in their work "Modeling the stress state of reinforced specimens" [17] developed a mathematical model of the stress state of ice reinforced with geosynthetic materials. In this model, using the finite difference method, normal and shear stresses in the samples are calculated. However, the Hoek–Brown model is missing in the work [8]. There are several methods for thermodynamic modeling of ice; for example, the article by Y. Fang describes the model based on the Winton model, which takes into account the influence of snow cover, vertically changing ice salinity, and an increased number of layers considered [18]. Also, a thermodynamic model was considered in the article by J. Zhao on the effect of snow cover on the thickness of sea ice in Prydz Bay, East Antarctica [19]. In the article by M. Prasanna about laboratory experiments on the destruction of floating salt ice blocks in contact with ice, an experimental system for studying the nature of ice destruction is considered [20]. Thermodynamic modeling of the consolidated ice hummock layer using the Comsol Multiphysics software package is described in the articles by E. Salganik [21, 22]. This model also can be found in some works about structure "freeze-in the ice" [23, 24]. In C. Pang's article, the determination of the initial nature of the fracture during ice bending was considered and the numerical model of the ice field "Fixed effects" model was considered [25]. M. Mokhtari modeled ice in the computer program "VUMAT" and "Crushable Foam" to analyze its plastic properties during crushing [26]. There are several natural experiments to determine ice loads on structures, such as the article by Å. Ervik on the interaction of hummocks with lighthouses and the assessment of global ice loads [27]; in the article by M. van den Berg, a study was conducted on the interaction of ice with vertical-type structures [28]. T. Kärnä considered numerical modeling to determine the ice load on structures [29].

The relevance of the study lies in the lack of practical information on applying the Hoek–Brown model to solving problems of ice destruction by bending. There was no Hoek–Brown model considered for calculating the strength characteristics of ice in the known literature above. The most common models that should be taken into account when choosing a material model in general case are (using the Plaxis software package): linear model, Mohr-Coulomb model, Hardening soil model, Soft soil model, Jointed rock model, Hoek–Brown model. It should be noted that there are other models [30], but they are not presented by default in the considered software package. Linear elasticity model: this model assumes that the behavior of the material is linear and elastic, which means that the relationship between stress and strain is proportional and that the ice returns to its original state after the load is removed. Mohr-Coulomb model: this model is used for a material under shear loads, and it takes into account the relationship between shear stress and normal stress. Hardening Soil Model: this model assumes the strengthening effect of both compressive and shear soil. The stiffness characteristics of the material model increase with increasing pressure. Model of Weakly(small) Hardening soil takes into account the elastic behavior of the material during unloading and its reloading at small deformations. The Rock model is an anisotropic model of the behavior of fractured rock and is a linearly elastic and ideally plastic model. Reduced elastic and plastic properties can only occur in shear planes. The Hoek–Brown model, an isotopically ideal-plastic linear elastic model, which is characterized by the Hoek–Brown strength criterion, which consists in a nonlinear dependence of stresses, characterizes the moment of occurrence of plastic deformations. The described material models use different initial data, which must also be taken into account when preparing the calculation. A comparison of the initial data required for the calculation is given in Table 1.

Table 1. Initial data for different material models.

Model variable	Linear elastic	Mohr-Culomb	Hardening soil	Soft (weak) hardening soil	Rock	Hoek-Brown
E is Young's modulus, (for some models: E_{50ref} , $E_{ref oed}$, $E_{ref ur}$)	+	+	+	+	+	+
ν is Poisson's ratio	+	+	+	+	+	+
φ is angle of friction or effective angle of friction		+	+	+	+	
c is cohesion coefficient or effective cohesion coefficient		+	+	+	+	
ψ is dilatancy angle		+	+	+	+	+
σ_t is tensile limit and tensile strength		+	+	+	+	
ΣC_i is uniaxial compressive strength of undisturbed soil						+
m_i is intact rock parameter						+
GSI is Geological strength index						+
D is disturbance factor						+
N is number of crack directions					+	
$\alpha_{1,i}$ is dip angle ($-180^\circ \leq \alpha_{1,i} \leq 180^\circ$)					+	
α_{2i} is stretch ($-180^\circ \leq \alpha_{1,i} \leq 180^\circ$), ($\alpha_{2i}=90^\circ$ PLAXIS 2D)					+	
$G_{0 ref}$ is shear modulus at ultrasmall strains				+		
$\gamma_{0.7}$ is strain threshold ($G_s=0.722G_0$)				+		
m is exponent for the dependence of stiffness on the stress level			+			

The data presented in the table clearly demonstrate that some material models have a minimum amount of initial data. The Hoek–Brown model, in comparison with the linear model, also takes into account: the uniaxial compressive strength of the undisturbed soil, the parameter of the undisturbed soil, the geological strength index, the coefficient of disturbance as input data. There are practical and theoretical methods of analysis to select the appropriate material model. Theoretical ones include the analysis of the mathematical model of the behavior of the ice material and the selection of the maximum correspondence with the known model in the given boundary conditions. A practical way of analysis includes comparing models with the results of natural experiments. When choosing a theoretical approach, it makes sense to consider the Brugers model, Fig. 1 [31]. This model consists of "Maxwell Units" and "Kelvin Units". The Maxwell unit is responsible for the viscoplastic behavior of the material, and the Kelvin unit is responsible for the partial recovery after loading. This model makes it possible to take into account the rate of ice deformation, which is an important factor for a certain category of tasks.

**Figure 1. Brugers model for ice [31].**

In the Fig. 1: E_1 is Young's modulus for "Maxwell Unit", E_2 is Young's modulus for "Kelvin Units", η_1 and η_2 are viscosity factor for the corresponding unit.

The Brueger model describes the behavior of ice; however, in practical calculations, it makes sense to reduce the number of degrees of freedom by setting certain restrictions and assumptions, such as a known strain rate, which makes it possible to significantly simplify the model. When choosing a practical approach to model selection based on direct experiments, it is important to have a sufficient amount of initial experimental data. For further analysis, the work used the initial data based on the experiments of M. Karulina [11, 12] presented in Table 2.

Table 2. Initial data for analysis.

No.	Length, m	Width, m	Thickness, m	Salinity, ppt	Temperature, °C	Bending strength, kPa	Date	Place
1	1.97	0.64	0.23	5.57	-8.00	346.7		
2	1.27	0.58	0.22	5.57	-8.00	258.3	05.03.2010	
3	1.40	0.56	0.22	5.57	-8.00	302.6		
4	1.38	0.56	0.22	5.57	-8.00	256.7		Tempel fjord
5	1.90	0.74	0.35	5.57	-5.18	310.5	06.03.2010	
6	1.98	0.68	0.35	5.57	-5.18	281.8		
7	2.50	0.51	0.51	6.03	-3.77	213.2	07.03.2010	
8	2.53	0.58	0.49	5.78	-3.90	282.3	19.02.2011	
9	3.39	0.50	0.45	3.50	-2.10	169.0		
10	2.13	0.48	0.40	2.70	-1.40	149.8		
11	2.30	0.46	0.39	2.70	-1.60	186.1	03.05.2010	Van Mijen fjord
12	2.27	0.45	0.37	5.70	-2.20	131.6		
13	3.02	0.60	0.49	3.90	-2.10	128.1		
14	1.22	0.25	0.23	7.72	-3.20	202.0	25.02.2011	Advent fjord
15	1.33	0.27	0.25	7.72	-3.20	160.8		
16	1.59	0.45	0.31	5.96	-2.30	193.0		
17	2.40	0.68	0.40	6.98	-2.00	205.0	21.03.2012	
18	2.22	0.45	0.31	8.38	-2.20	178.0		Sveagruva
19	3.40	0.63	0.63	4.53	-6.50	186.0	26.03.2012	
20	3.18	0.63	0.65	3.30	-3.30	328.0	28.03.2012	

These results were obtained during experiments in the fjords of Svalbard and published in the journal [3]. The values presented in the table were used to justify the possibility of using the Hoek–Brown model to calculate the destruction of ice by bending in the Plaxis software package, which was the purpose of this work.

The goals of this work are:

1. Analyze the Hoek–Brown model for calculations related to the flexural stiffness of ice.
2. Analyze the possibility of calculation using the Plaxis software product (Hoek–Brown model in the list of available standard models).
3. Carry out a series of numerical calculations using the Hoek–Brown model and compare them with the results of physical experiments carried out in the field. Assess the error/convergence of numerical and field experiments.
4. Assess the possibility of using the Vaudrey equation [32] for ice models.

2. Methods

Numerical models were created in a finite element software package for the verification of the Hoek–Brown model for the calculations of the flexural strength of ice. The calculation results were analyzed and compared with the actual results of physical experiments.

The flexural test of ice is a classic traditional field test for hydrological surveys. During experiments to determine the strength of ice in bending in the field, the ice beam is sawn from three sides (one side is connected to the original ice level), then loads are applied to one end of the beam, and deformations are fixed until the moment of destruction, Fig. 2 [11].



Figure 2. Field experiment to determine the bending strength of a beam [12].

It is assumed that the embedment of the beam is rigid and that the Archimedes force does not affect the result of the experiment. There are "MAGI" recommendations, which regulate the dimensions of beams depending on their thickness in order to reduce the effect of shift/variations on the result [33]. The 'rate of load increase' is chosen in such a way that no more than 1–2 seconds elapse from the beginning of the process of applying the load to the destruction of the beam. The advantage of this test method is undisturbed structure of the sample; the disadvantage of this method is the possible formation of stress concentrations at the site of the ice beam.

Fig. 3 shows an example of a graph of the dependence of the beam deformation on the load [12].

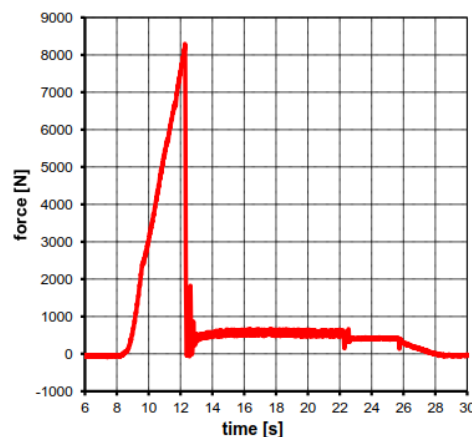


Figure 3. Force dependence on time for determining the bending strength of a beam [12].

The numerical formulation of the experiment was implemented in the Plaxis software package in 2D. Plaxis is a modern software package for performing calculations, mainly related to soil and foundations. The program is based on the finite element method. The entire computational area (within the given boundaries) is divided into a certain number of connected mesh elements, and the required values are determined at the nodes (depending on the type of element) of the mesh. The mesh element size was determined by practical considerations, taking into account the necessary absence of influence on the result. The default recommended model boundary conditions were used, which restrict horizontal movements at the lateral boundaries of the model and restrict vertical movements at the bottom boundary of the model. For a 2D setting, the boundary conditions take the following form (x is the horizontal axis, y is the vertical axis).

The vertical boundaries of the model allow vertical displacements, but they are fixed in the direction normal to the vertical side boundary [9].

$$u_x = 0, \quad u_y = \text{free}. \quad (1)$$

The "bottom" of the model is fixed in all directions.

$$u_x = u_y = 0. \quad (2)$$

The "top surface" is free in all directions.

$$u_x = \text{free}, u_y = \text{free}. \quad (3)$$

Fig. 4 shows the calculation model in the software package.

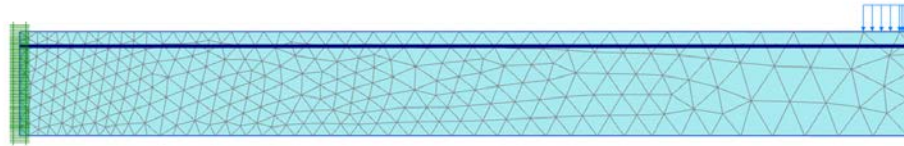


Figure 4. Calculation model.

The presented model contains: 579 elements, 4851 nodes. The dimensions of the simulated beam were selected according to known field test results.

The following parameters were used in the calculation:

Young's modulus (E) is a physical quantity that characterizes the ability of a material to resist compression and tension during elastic deformation. In the Hoek–Brown model, Young's modulus is determined depending on the quality of the rock.

Poisson's ratio (ν) characterizes the ratio of transverse deformation of the material during its tension or compression.

Undisturbed uniaxial compressive strength (σ_{ci}) is the ratio of the vertical load applied to a material sample at which its destruction occurs to its cross-sectional area.

Undisturbed rock parameter (m_i) is an empirical parameter that depends on the type of rock being tested.

The Geological Strength Index (GSI) is a parameter that takes into account the nature of the fracture of the rock and the "blockiness" of the massif.

Disturbance coefficient (D) is a parameter characterizing the degree of rock damage as a result of mechanical impact.

The geological strength index and the failure coefficient were taken as $GSI = 100$, $D = 0$, taking into account the fact that the beams were sawn in natural conditions and should not undergo changes in temperature and salinity during testing.

The m_i parameter was selected taking into account the greatest convergence with the experimental data, $m_i = 7$.

The load at which the ultimate bending strength of the beam was calculated is derived from the equation:

$$\sigma_f = \frac{6Pl}{bh^3}, \quad (4)$$

where σ_f is beam bending strength limit, P is load applied to the beam, kN; l is beam length, m; b is beam width, m; h is beam height, m.

Formula (4) represents the ratio of the load to the moment of resistance, resulting in the ultimate bending stress that the material can withstand.

Young's modulus of elasticity (E) for sea ice was determined by the Vaudrey equation [32], according to experimental data. This equation is included in ISO 19906 [2]:

$$E = 5.31 - 0.436\sqrt{v_b}, \quad (5)$$

where v_b is liquid brine content of sea ice, ‰.

The brine volume is calculated depending on the temperature, T , °C and salinity of sea ice, S , ‰ [34]:

$$v_b = S \left(\frac{49.185}{|T|} + 0.532 \right). \quad (6)$$

Poisson's ratio was calculated as a function of temperature according to the equation proposed by Wicks and Assour:

$$v = 0.33 + 0.06105 \exp\left(\frac{T}{5.48}\right). \quad (7)$$

The density of ice depends on temperature, pressure, salinity and other factors. The dependence of ice density on temperature T and pressure P is given by the following empirical equation:

$$\rho(P, T) = \rho_0 \left[1 + 0.94 \cdot 10^{-7} \left(\frac{P}{1.01 \cdot 10^5} - 1 \right) \right] (1 - 1.53 \cdot 10^{-4} T). \quad (8)$$

The strength of ice for uniaxial compression was obtained according to Russian normative document SP 38.13330.2018 [3] depending on the temperature and salinity of the ice. The type of ice crystal structure was assumed to be granular.

The load specified in the software package is calculated from equation (4) based on experimental data.

Initial data doesn't have pressure details for each sample therefore the pressure is assumed to be constant and equal to normal atmospheric pressure.

The PLAXIS software package solves a two-dimensional problem, taking into account the fact that the load was recalculated for the beam of a certain width. The specified load was reduced to a value of one meter, taking into account the width of the beams. In the calculation model, the water level is set at a ratio of 0.9 from the thickness of the surrounded level ice. An example of a calculation scheme is shown in Fig. 4. An example of the characteristics used for the Hoek–Brown model is given in Table 3.

Table 3. Example of characteristics used for the Hoek–Brown model.

Characteristic	Value	Units
γ	8.99	kN/m ³
E	2650000	kN/m ²
ν	0.347	–
σ_{ci}	2054	kN/m ²
m_i	7.0	–
GSI	100.0	–
D	0.00	–

A data array was prepared for the calculation model based on the described expressions, Table 4.

Table 4. Data for the calculation model

No	Length, m	Width, m	Thickness, m	Salinity, S , ‰	Temperature, T , °C	Strength, σ_f , kPa	Load, P , kN	Recalculated load, P , kN/m	Brine volume, v_b , ‰	Modulus of elasticity, E , GPa	Poisson's ratio, ν	Ice density, ρ , kg/m ³	σ_{ci} , MPa
1	1.97	0.64	0.23	5.57	-8.00	346.70	0.993	1.552	37.208	2.650	0.347	916.80	2.054
2	1.27	0.58	0.22	5.57	-8.00	258.30	0.952	1.641	37.208	2.650	0.347	916.80	2.054
3	1.40	0.56	0.22	5.57	-8.00	302.60	0.976	1.744	37.208	2.650	0.347	916.80	2.054
4	1.38	0.56	0.22	5.57	-8.00	256.70	0.840	1.501	37.208	2.650	0.347	916.80	2.054
5	1.90	0.74	0.35	5.57	-5.18	310.50	2.469	3.337	55.851	2.052	0.357	916.80	1.512

No	Length, m	Width, m	Thickness, m	Salinity, S , ‰	Temperature, T , °C	Strength, σ_f , kPa	Load, P , kN	Recalculated load, P , kN/m	Brine volume, V_b , ‰	Modulus of elasticity, E , GPa	Poisson's ratio, ν	Ice density, ρ , kg/m ³	σ_{ci} , MPa
6	1.98	0.68	0.35	5.57	-5.18	281.80	1.976	2.906	55.851	2.052	0.357	916.80	1.512
7	2.50	0.51	0.51	6.03	-3.77	213.20	1.885	3.697	81.878	1.365	0.364	916.80	1.195
8	3.39	0.50	0.45	3.50	-2.10	169.00	0.841	1.683	83.837	1.318	0.375	916.80	1.253
9	2.13	0.48	0.40	2.70	-1.40	149.80	0.900	1.875	96.293	1.032	0.380	916.80	1.603
10	2.30	0.46	0.39	2.70	-1.60	186.10	0.944	2.051	84.436	1.304	0.379	916.80	1.644
11	2.27	0.45	0.37	5.70	-2.20	131.60	0.595	1.323	130.466	0.330	0.374	916.80	0.925
12	3.02	0.60	0.49	3.90	-2.10	128.10	1.018	1.697	93.418	1.096	0.375	916.80	1.135
13	2.53	0.58	0.49	5.78	-3.90	282.30	2.590	4.465	75.970	1.510	0.363	916.80	1.247
14	1.22	0.25	0.23	7.72	-3.20	202.00	0.365	1.460	122.766	0.479	0.367	916.80	0.777
15	1.33	0.27	0.25	7.72	-3.20	160.80	0.340	1.259	122.766	0.479	0.367	916.80	0.777
16	1.59	0.45	0.31	5.96	-2.30	193.00	0.875	1.944	130.624	0.327	0.373	916.80	0.917
17	2.40	0.68	0.40	6.98	-2.00	205.00	1.549	2.278	175.369	0.464	0.375	916.80	0.715
18	2.22	0.45	0.31	8.38	-2.20	178.00	0.578	1.284	191.808	0.728	0.374	916.80	0.539
19	3.40	0.63	0.63	4.53	-6.50	186.00	2.280	3.619	36.688	2.669	0.352	916.80	1.925
20	3.18	0.63	0.65	3.30	-3.30	328.00	4.576	7.263	50.941	2.198	0.366	916.80	1.576

Remark: Colored rows correspond to the values with significant relative mistake obtained

3. Results and Discussion

The calculations were carried out for a previously prepared data array based on the initial data from the experiments of M. Karulina [11, 12]. Fig. 5 shows the deformed scheme of the calculation model. Fig. 6 shows the bending moment in a cantilever beam.

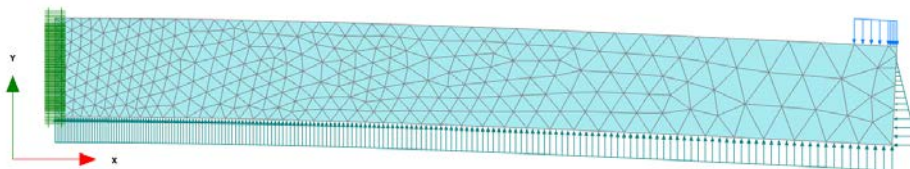


Figure 5. Deformed scheme of the model.

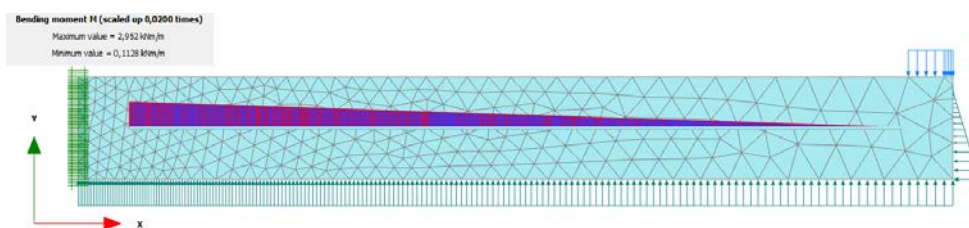


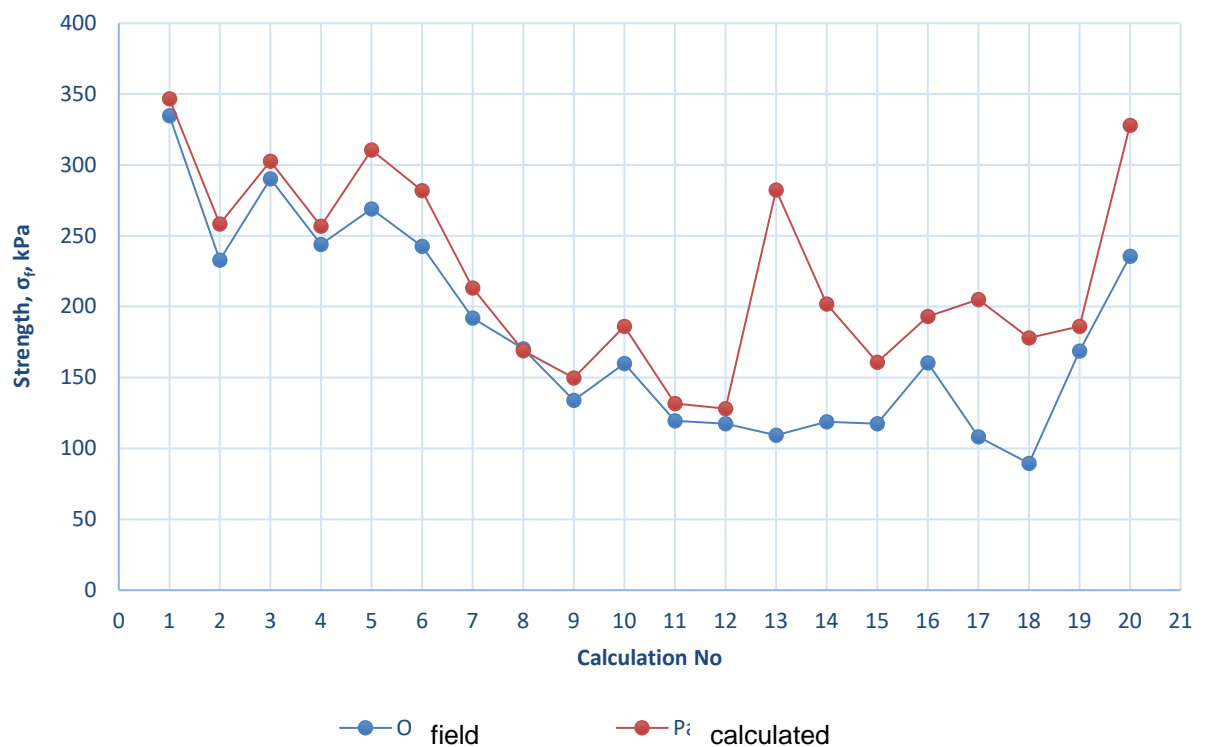
Figure 6. Bending moment in a beam.

The resulting nature of displacements and the dependence of the moment correspond to the expected ones, which were published in the work [11, 12]. The bending moment per one meter length was recalculated to the experimental width of the beam, and the strength was calculated by formula (4).

Table 5 shows the results of calculations and the variation between the strength characteristics obtained empirically and modeled in the software package [8]. In Fig. 7, the results are presented in the form of graphs.

Table 5. Comparisons of results.

No	Bending moment, kNm /m	Recalculated moment, kNm	Strength, kPa	Strength, kPa (experimental data)	Variation
1	2.952	1.889	334.82	346.70	4%
2	1.878	1.089	232.81	258.30	11%
3	2.342	1.312	290.33	302.60	4%
4	1.968	1.102	243.97	256.70	5%
5	5.491	4.063	268.95	310.50	15%
6	4.952	3.367	242.55	281.80	16%
7	8.318	4.242	191.88	213.20	11%
8	5.750	2.875	170.37	169.00	1%
9	3.569	1.713	133.84	149.80	12%
10	4.051	1.863	159.80	186.10	16%
11	2.725	1.226	119.43	131.60	10%
12	4.701	2.821	117.48	128.10	9%
13	4.372	2.536	109.25	282.30	158%
14	1.047	0.262	118.75	202.00	70%
15	1.224	0.330	117.50	160.80	37%
16	2.570	1.157	160.46	193.00	20%
17	2.883	1.960	108.11	205.00	90%
18	1.433	0.645	89.47	178.00	99%
19	11.160	7.031	168.71	186.00	10%
20	16.580	10.445	235.46	328.00	39%

**Figure 7. Comparison of the strength of ice based on the calculation results.**

An analysis of the results shows that some of the deformation modulus obtained with Vaudrey equation (5) [2] have a negative value, which is associated with a large volume of brine contained in the sea ice.

The density of sea ice does not change when determining by using formula (8) [34], which takes into account temperature and pressure.

The largest variation of results was for the experiments No. 13,14,18,20 (Table 5). Possible error reaches a value of 50 %.

Some results of experiments (No 17, 18) can be explained by the deviation of the deformation modulus, which is probably associated with a large volume of brine in the ice structure, since the results were obtained at a relatively high ice temperature and high salinity.

In Karulina's experiments [11, 12], a comparison was made to determine the bending strength of ice obtained experimentally with empirical formulas depending on the volume of brine. There is also a discrepancy in some results, which is due to the internal structure of the ice depending on a certain region [2]. This could be an explanation for big discrepancy of the experiment No 13, as the location of the data sample is different. Location and brine volume influence on the result was also discussed by Marchenko in the article "Experimental studies of sea ice elastic behavior" [31]. The study revealed the dependence of the deformation modulus on the volume of brine in ice, which explains the big variation for experiment No 13.

4. Conclusions

1. In the work, the Hoek–Brown model for calculations related to the flexural stiffness of ice was analyzed. The results of the Hoek–Brown model showed the possibility of its application in the general case; however, it is necessary to carefully monitor the deviation of the initial and resulting data; one of the reasons for the result discrepancy could be a variation of the brine volume in ice. Arctic engineering projects generally include a field research stage when the properties of ice in situ could be examined and a correction to the material model could be introduced.

2. Plaxis software product was used, and therefore calculations were limited to the available models and functions in this software. The study showed that the Hoek–Brown model available in the Plaxis software package can be used. No fundamental limitations were found in the program. However, ice has a significant variation of properties (including brine volume), which should be considered in the model. Therefore, it is difficult to build a simple unique ice model for all locations.

3. A significant series of numerical experiments was carried out and compared with the results obtained in the field. In most cases, the convergence of the results was revealed, with an error that in most cases does not exceed 20 %. The bigger discrepancy (40 %) for some result points can be explained due to the presence of excessive brine volume in ice. Variations in the field data are a subject of separate studies of statistical inhomogeneity. The present deviation was considered acceptable for the purpose of this work. It should be noted that for field experiments related to the properties of ice, the results often vary by several times [12].

4. Based on the analyzed data, it can be seen that the dependence of the Young's modulus on the Vaudrey equation [32] is not applicable to all ice models. However, it is a convenient calculation method, which provides acceptable results for most cases. Based on the results obtained, it is possible to estimate a variation of the result to introduce a correction factor, which will allow using the described model with the prescribed level of reliability.

References

1. API-RP-2N Recommended practice for planning, designing, and constructing structures and pipelines for arctic conditions. American Petroleum Institute, 1995.
2. DS/ISO 19906-2019 Petroleum and natural gas industries – Arctic offshore structures. International Organization for Standardization, 2010.
3. Russian Code Specification SP 38.13330.2018 Loads and impacts on hydraulic structures (from wave, ice and ships). – Moscow: Ministry of Regional Development of Russia, 2018.
4. NORSOK STANDARD N-003 Actions and action effects. 2007.
5. Timco, G.W., Croasdale, K.R. How well can we predict ice loads. Proceedings of the 18th IAHR International Symposium on Ice. 2006. Pp. 167–174.
6. Frederking, R. Comparison of standards for predicting ice forces on arctic offshore structures. Proceedings of the Tenth (2012) ISOPE Pacific/Asia Offshore Mechanics Symposium. Vladivostok, Russia, 2012.
7. Shkhinek, K., Blanchet, D., Croasdale, K., Matskevitch, D.G., Bhat, S. Comparison of the Russian and foreign codes and methods for global load estimation. Book Comparison of the Russian and Foreign Codes and Methods for Global Load Estimation. 1994. Pp. 75–81.
8. Material Models Manual PLAXIS CONNECT Edition V20, Build 10265. Bentley, 2020.
9. Scientific Manual PLAXIS CONNECT Edition V20, Build 10265. Bentley, 2020.

10. Peng, C. Eksperimental'nyye issledovaniya i analiz kharakteristik predela prochnosti morskogo l'da na izgib vdol' poberezh'ya Bokhayskogo zaliva [Experimental studies and analysis of the characteristics of the bending strength of sea ice along the coast of the Bohai Bay]. *Molodoy uchonyy*. 2017. 27 (161). Pp. 39–46. (rus)
11. Karulina, M., Marchenko, A., Karulin, E., Sodhi, D., Sakharov, A., Chistyakov, P. Full-scale flexural strength of sea ice and freshwater ice in Spitsbergen Fjords and North-West Barents Sea. *Applied Ocean Research*. 2019. 90 (C10). 101853. DOI: 10.1016/j.apor.2019.101853
12. Karulina, M., Karulin, E., Marchenko, A. Field investigations of first year ice mechanical properties in North-West Barents Sea. *Proceedings of the International Conference on Port and Ocean Engineering under Arctic Conditions. POAC 2013*, 2013.
13. Sodhi, D.S. Vertical penetration of floating ice sheets. *International Journal of Solid and Structures*. 1998. 35 (32–32). Pp. 4275–4294.
14. Vasiliev, N.K., Karulina, M.M., Marchenko, A.V., Sakharov, A.N., Chistyakov, P.V. Ispytaniya konsoly armirovannogo morskogo l'da [Reinforced sea ice cantilever testing]. *Izvestiya VNIIG im. B.E. Vedeneeva*. 2015. 277. Pp. 46–55.
15. Li, L., Shkhinek, K. The ultimate bearing capacity of ice beams. *Magazine of Civil Engineering*. 2013. 1 (36). Pp. 65–74. DOI: 10.5862/MCE.36.8
16. Godetsky, S.V., Kokin, O.V., Kuznetsova, O.A., Tsvetsinsky, A.S., Arhipov, V.V. Estimation of ice strength limits for uniaxial compression in the Sea of Okhotsk according to measurements and calculations. *Ice and Snow*. 2021. 61 (4). Pp. 561–570. (rus). DOI: 10.31857/S2076673421040108
17. Yakimenko, O.V., Matveev, S.A. Modelirovaniye napryazhenogo sostoyaniya armirovannykh ledovykh obraztsov-balok [Simulation of the stress state of reinforced ice specimens-beams]. *Vestnik SibADI*. 2011. 3 (21). Pp. 39–44. (rus)
18. Fang, Yo., Wu, T., Hu, A., Chu., M. A modified thermodynamic sea ice model and its application. *Ocean Modelling*. 2022. 178 (1). 102096. DOI: 10.1016/j.ocemod.2022.102096
19. Zhao, J., Cheng, B., Vihma, T., Yang, Q., Hui, F., Zhao, B., Hao, G., Shen, H., Zhang, L. Observation and thermodynamic modeling of the influence of snow cover on landfast sea ice thickness in Prydz Bay, East Antarctica. *Cold Regions Science and Technology*. 2019. 168 (C11). 102869. DOI: 10.1016/j.coldregions.2019.102869
20. Prasanna, M., Wei, M., Polojärvi, A., Cole, D.M. Laboratory experiments on floating saline ice block breakage in ice-to-ice contact. *Cold Regions Science and Technology*. 2021. 189. 103315. DOI: 10.1016/j.coldregions.2021.103315
21. Salganik, E., Høyland, K.V., Shestov, A. Medium-scale experiment in consolidation of an artificial sea ice ridge in Van Mijenfjorden, Svalbard. *Cold Regions Science and Technology*. 2021. 181. 103194. DOI: 10.1016/j.coldregions.2020.103194
22. Salganik, E., Høyland, K.V., Maus, S. Consolidation of fresh ice ridges for different scales. *Cold Regions Science and Technology*. 2020. 171. 102959. DOI: 10.1016/j.coldregions.2019.102959
23. Sharapov, D., Shkhinek, K., DelValls, T.Á. Ice collars, development and effects. *Ocean Engineering*. 2016. 115. Pp. 189–195. DOI: 10.1016/j.oceaneng.2016.02.026
24. Sharapov, D., Shkhinek, K. Numerical calculation of the ice grow and empirical calculation results. *Advanced Materials Research, Proceedings of 3rd International Conference on Materials and Products Manufacturing Technology (ICMPMT 2013)*. September 25–26, Changsha, China, 2013.
25. Pan, C., Peng, D., Xu, N., Wang, Y. Determination of initial breaking pattern in the bending failure of a semi-infinite ice sheet. *Polar Science*. 2022. 34. 100869. DOI: 10.1016/j.polar.2022.100869
26. Mokhtari, M., Kim, E., Amdahl, J. Pressure-dependent plasticity models with convex yield loci for explicit ice crushing simulations. *Marine Structures*. 2022. 84. 103233. DOI: 10.1016/j.marstruc.2022.103233
27. Ervik, Å., Nord, T.S., Høyland, K.V., Samardzija, I., Li, H. Ice-ridge interactions with the Norströmsgrund lighthouse: Global forces and interaction modes. *Cold Regions Science and Technology*. 2019. 158. DOI: 10.1016/j.coldregions.2018.08.020
28. Berg, M., Owen, C.C., Hendrikse, H. Experimental study on ice-structure interaction phenomena of vertically sided structures. *Cold Regions Science and Technology*. 2022. 201. DOI: 10.1016/j.coldregions.2022.103628
29. Kärnä, T., Kamesaki, K., Tsukuda, H. A numerical model for dynamic ice–structure interaction. *Computers & Structures*. 72 (4–5). Pp. 645–658.
30. Schulson, E.M. Brittle failure of ice. *Engineering Fracture Mechanics*. 2001. 68 (17–18). Pp. 1839–1887.
31. Marchenko A. V., Karulin Y. B., Chistyakov P. V. Experimental studies of sea ice elastic behavior. *Vesti Gazovoy Nauki: collected scientific technical papers*. 2020. 3 (45). Pp. 129–140.
32. Vaudrey, K. Ice engineering – study of related properties of floating sea ice sheets and summary of elastic and viscoelastic analysis: Rep. TR860. Port Huenem, CA: U.S. Naval Civil Engineering Lab., 1977.
33. Maattanen, M. On the flexural strength of brackish water ice by in situ tests. *Mar. Sci. Comuns*. 1976. 2 (2). Pp. 125–138.
34. Sharapov D. Freezing into ice of sea and river hydraulic engineering structures. Saint-Petersburg: Peter the Great St.Petersburg Polytechnic University, 2023. P.167. DOI: 10.18720/SPBPU/2/i23-240

Information about authors:

Sofiya Andreeva,

E-mail: Cofiaand16@gmail.com

Dmitry Sharapov, PhD

ORCID: <https://orcid.org/0000-0001-8650-2375>

E-mail: sharapov.dm@gmail.com

Received 08.03.2023. Approved after reviewing 24.08.2023. Accepted 24.08.2023.